AN INVESTIGATION OF MANTLE RAYLEIGH WAVES*

By MAURICE EWING and FRANK PRESS

ABSTRACT

Dispersion of Rayleigh waves for a new range of periods ranging from 1 to 7 minutes is described. The group velocity curve shows a long-period and a short-period branch merging at a minimum value of 3.54 km/sec. with a corresponding period of about 225 sec. It is suggested that the known variation of velocity with depth in the mantle can account for the observed dispersion. The small scatter in the velocities and the absorption of these waves suggests that, unlike shorter-period surface waves, refraction and attenuation effects are negligible at the continental margins. From the absorption of mantle Rayleigh waves the internal friction in the upper mantle for periods of 140 and 215 sec. is found to be given by $1/Q = 670 \times 10^{-5}$. This is of the same order as that reported from vibration measurements at audio frequencies on laboratory samples of crystalline rocks at normal pressure and temperature.

INTRODUCTION

THE PRESENT study of the Rayleigh waves in the period range of 1 to 7 minutes was made possible through the coöperation of Professor H. Benioff, who brought to the author's attention the long Rayleigh waves recorded at Pasadena for the three earthquakes considered. The first of these is the great Assam earthquake of 15 August 1950. According to B.C.I.S. the epicenter is 28°.6 N, 96°.5 E, origin time 14:09:30. The Pasadena magnitude was 8.6, epicentral distance 109°.5, and azimuth of the epicenter N 32° W. The Rayleigh waves R_3, R_4, R_5, R_7, which B. Gutenberg had reported in the Pasadena Bulletin, were read for a wide range of periods on the long-period Benioff vertical and north–south seismographs and on the north–south linear strain seismograph. The second earthquake was the Japanese shock of 2 March 1933. According to I.S.S. the epicenter is 39°.1 N, 144°.7 E, origin time 17:31:01. The Pasadena magnitude was 8.5, epicentral distance 74°.1, and azimuth of the epicenter N 58° W. The Rayleigh waves R_2, R_3, R_4 were read on the north–south linear strain seismograph. The third earthquake studied was the Tonga shock of 8 September 1948, which according to J.S.A. occurred at 21°.0 S, 174°.2 W, origin time 15:09:14. The Pasadena magnitude was 8, epicentral distance 76°.8, and azimuth of the epicenter S 53° W. Only R_2 could be read for this earthquake on the long-period Benioff vertical seismograph.

Although the paths of the Rayleigh waves involve as much as three complete passages around the earth, the orbital motion of a surface particle could be demonstrated to be proper for Rayleigh waves and the group velocities deduced from all the paths could be represented by a single dispersion curve whose broad features may be accounted for in terms of mantle structure.

The investigation of Rayleigh-wave dispersion in the period range 1 to 7 minutes represents a new field of study, since most previous studies have been devoted to waves with periods less than about 50 sec. Many writers have made deductions of crustal structure from the observed Rayleigh-wave dispersion curves, and the

* Manuscript received for publication October 20, 1952.
This research has been supported by the Geophysics Research Division of the Air Force Cambridge Research Center under Contract AF 19(122)441.

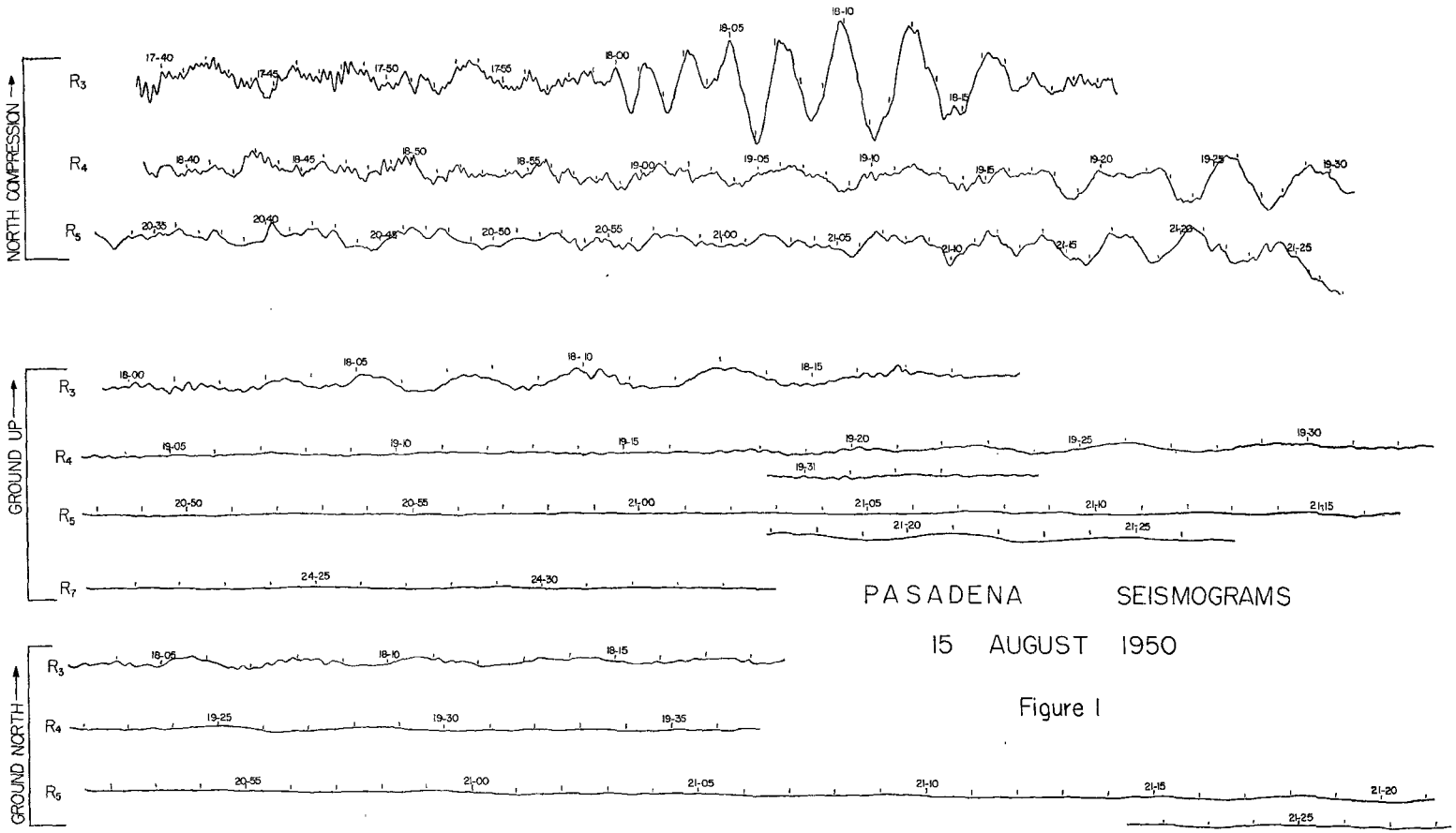

Fig. 1. Tracings of the Pasadena N–S linear strain (T_g = 70 sec.), vertical and N–S (T_0 = 1 sec., T_g = 90 sec.) seismographs for the earthquake of 15 August 1950.

TABLE 1

R_3 ARRIVAL TIMES FOR MAXIMUM AND MINIMUM TRACE DEFLECTION, 15 AUGUST 1950

Short-period branch				Long-period branch		
Phase		Uncorrected arrival time (G.C.T.)	Ground amplitude (mm.)	Phase		Uncorrected arrival time (G.C.T.)
U		17:59:38		R		17:39:04
	C	18:00:02			C	41:50
	D	00:18		R		44:24
R		00:40			C	47:20
U		00:50		R		51:14
	C	01:17			C	53:25
	D	01:37		R		56:20
R		02:14			C	58:32
U		02:22		R		18:01:16
	C	03:12			C	03:55
	D	03:25	0.36	R		06:00
S		03:51			C	09:00
	R	04:02				
	U	04:21	0.44			
N		04:43				
	C	05:00				
	D	05:19	0.82			
S		05:38				
	R	06:04				
	U	06:22	0.94			
N		06:43				
	C	07:18				
	D	07:32	1.3			
S		07:57				
	R	08:31				
	U	08:43	1.5			
N		09:16				
	C	09:50				
	D	10:04	3.0			
S		10:43				
	R	11:20				
	U	11:32	4.2			
N		12:28				
	C	13:00				
	D	13:12	4.2			
S		14:12				
	R	14:44				
	U	15:02	3.6			
N		15:49				
	C	16:28				
	D	16:37				
S		17:27				
	U	18:30				
D		20:25				

TABLE 2
R_4 ARRIVAL TIMES FOR MAXIMUM AND MINIMUM TRACE DEFLECTION,
15 AUGUST 1950

Short-period branch				Long-period branch			
Phase		Uncorrected arrival time (G.C.T.)	Ground amplitude (mm.)	Phase		Uncorrected arrival time (G.C.T.)
C		19:15:36		R		18:40:00
	R	16:28			C	43:16
C		17:36		R		47:00
D		17:35	0.38		C	49:40
	R	18:46		R		53:00
	U	18:54	0.44		C	55:38
C		19:54		R		58:20
D		20:14	0.44		C	19:01:04
	R	21:16		R		04:00
	U	21:16	0	U		03:48
C		22:38			C	06:26
D		22:37	0.68		D	06:36
	N	23:06		R		08:54
R		23:52		U		09:25
U		24:17	1.7		C	11:52
	S	24:56			D	12:17
C		25:34		R		14:08
D		25:53	2.8	U		14:12
	N	26:32			C	16:36
R		27:24		R		18:40
U		27:40	2.2		C	21:20
	S	28:21				
C		29:28				
D		29:21	1.5			
	N	30:21				
U		31:46	0.8			
	S	32:43				
D		33:21				
	N	34:36				
S		36:44				

general conclusion is that the sialic rocks of the continents extend to a depth of about 40 km. and that they are essentially absent under the oceans. Wilson and Baykal[1] have presented the most recent dispersion curve for continents covering the period range 16 to 28 seconds. Ewing and Press[2] have presented dispersion curves for purely oceanic paths covering the period range 14 to 38 seconds, with velocities becoming less than half as large as those for the continents for some periods. The whole oceanic dispersion curve was quantitatively accounted for by allowance for the effect of the water layer on Rayleigh waves propagated in the underlying simatic rock.

[1] J. T. Wilson and Orhan Baykal, "Crustal Structure of the North Atlantic Basin as Determined from Rayleigh Wave Dispersion," *Bull. Seism. Soc. Am.*, 38: 41–53 (1948).

[2] Maurice Ewing and Frank Press, "Crustal Structure and Surface-Wave Dispersion, Part II: Solomon Islands Earthquake of 20 July 1950," *Bull. Seism. Soc. Am.*, 42: 315–325 (1952).

TABLE 3
R_5 ARRIVAL TIMES FOR MAXIMUM AND MINIMUM TRACE DEFLECTION, 15 AUGUST 1950

Short-period branch				Long-period branch			
Phase		Uncorrected arrival time (G.C.T.)	Ground amplitude (mm.)	Phase		Uncorrected arrival time (G.C.T.)
D		21:07:10		R		20:33:13
	U	08:07	0.16		C	35:36
D		09:03	0.18	R		38:32
	U	10:23	0.26		C	41:32
N		11:08		R		44:16
	C	11:45			C	47:00
	D	11:55	0.28	R		49:28
S		12:45		U		49:30
	R	12:47			N	52:12
	U	13:16	0.30	C		52:36
N		14:08		D		52:36
	C	14:07			S	54:25
	D	14:26	0.32	R		55:38
S		15:09		U		55:54
	R	15:40			N	56:36
	U	15:44	0.76	C		57:30
N		16:23		D		58:28
	C	17:22			S	59:04
	D	17:15	1.0	R		59:20
S		18:13		U		21:00:32
	R	18:50			N	01:28
	U	19:06	1.2	C		02:00
N		20:03		D		02:38
	C	20:28			S	04:15
	D	20:55	1.3	R		04:36
S		21:50		U		04:49
	R	22:44			N	06:50
	U	22:50	1.4	C		07:28
N		23:09		D		07:10
	D	24:34	0.74		R	09:50
S		25:31		C		11:44
	N	27:09				

The great contrast between continental and oceanic dispersion for periods less than 1 minute accounts for the bewildering variety of dispersion curves and the corresponding variety of general patterns of surface waves which have been obtained from mixed paths involving varying proportions of continental and oceanic segments. This contrast likewise causes strong effects of refraction and scattering at continental boundaries, thereby insuring that waves of periods less than 1 minute will be very weak, or absent, for paths such as the R_2, R_3, R_4 and R_7, which involve one or more complete trips around the earth and, in general, many passages across continental boundaries.

We consider that the short period limit of 1 minute for the long-period waves is

imposed by crustal structure, being the shortest wave length for which the continental and oceanic dispersion curves show no appreciable difference. The long-period limit of about 7 minutes is probably imposed by the seismometers, and seismometers capable of recording waves of longer period may be expected to carry Rayleigh-wave observations to the point where gravity and sphericity terms must be included and where the dimensions and properties of the core may be investigated.

DATA

In figure 1, tracings of the Pasadena long-period vertical and N–S (T_0 = 1 sec., T_g = 90 sec.) and the N–S linear strain (T_g = 70 sec.) seismograms are presented for the earthquake of 15 August 1950. The maximum and minimum deflections

TABLE 4

R_7 ARRIVAL TIMES FOR MAXIMUM AND MINIMUM TRACE DEFLECTION, 15 AUGUST 1950

Phase	Uncorrected arrival time (G.C.T.)	Ground amplitude (mm.)
U	24:23:04	
D	24:52	0.60
U	26:54	0.60
D	28:48	0.60
U	30:25	
D	32:12	
U	34:09	

were read for R_3, R_4, R_5, and R_7. A deflection on the vertical-component seismogram in the direction marked "ground up" relates to the response to an impulsive upward ground movement, as is customary. The same convention is followed for the N–S and the linear strain seismograms. For all readings made from these seismograms the waves are approximately sinusoidal, and with a minor exception the periods are well above those for the pendulums or galvanometers. Since the transducers and galvanometers are identical for all three instruments, one can discuss the phase relations by simply noting that the response of the pendulum is proportional to ground acceleration whereas the strain instrument responds directly to compressional and rarefractional strain.

Hence maximum trace deflections on each of the three instruments bear the same phase relationship as "ground down," "ground south," and "compression." For this reason ground motion corresponding to maximum trace deflection on the vertical, horizontal, and N–S strain seismographs will be denoted by D, S, C, respectively, and minimum trace deflections will be denoted by U, N, R.

Tables 1–4 give uncorrected arrival times for the maximum and minimum trace deflections indicated for the earthquake of 15 August 1950. Corrected time may be obtained by adding 23 seconds. It will be noted that the orbital motion, as indicated by the sequence of readings, is proper for Rayleigh waves from the north for R_3 and R_5, and from the south for R_4. R_7 could be read only on the vertical.

The arrival-time curves for the various orders of Rayleigh waves are shown in

TABLE 5
DISPERSION DATA FOR R_3, R_4, R_5, R_7, 15 AUGUST 1950

Uncorrected time[a] (G.C.T.)	Period (sec.)	Travel time (h:m:s)	Travel time (sec.)	Velocity (km/sec.)
		R_3—Δ = 52,210 km.		
17:42:00	370	03:32:53	12,773	4.09
17:50:10	344	03:41:03	13,263	3.94
17:57:30	316	03:48:23	13,703	3.81
18:04:00	292	03:54:53	14,093	3.70
18:09:10	274	04:00:03	14,403	3.62
18:13:20	240	04:04:03	14,643	3.57
18:17:50	226	04:08:43	14,923	3.50
18:18:00	220	04:08:53	14,933	3.50
18:14:10	212	04:05:03	14,703	3.55
18:11:00	190	04:01:53	14,513	3.60
18:08:30	158	03:59:23	14,363	3.64
18:06:20	132	03:57:13	14,233	3.67
18:04:20	120	03:55:13	14,113	3.70
18:02:30	102	03:53:23	14,003	3.73
18:00:50	86	03:51:43	13,903	3.76
17:59:50	69	03:50:43	13,843	3.77
		R_4—Δ = 67,890 km.		
18:43:30	402	04:34:23	16,463	4.12
18:50:10	360	04:41:03	16,863	4.03
18:57:00	338	04:47:53	17,273	3.93
19:04:30	312	04:55:23	17,723	3.83
19:12:10	296	05:03:03	18,183	3.73
19:19:20	274	05:10:13	18,613	3.65
19:25:20	248	05:16:13	18,973	3.58
19:31:50	240	05:22:43	19,363	3.51
19:32:10	232	05:23:03	19,383	3.50
19:27:40	224	05:18:33	19,113	3.55
19:24:20	208	05:15:13	18,913	3.59
19:22:00	158	05:12:53	18,773	3.62
19:20:00	142	05:10:53	18,653	3.64
19:17:50	136	05:08:43	18,523	3.67
19:16:20	124	05:07:13	18,433	3.68
		R_5—Δ = 92,240 km.		
20:38:00	342	06:28:53	23,333	3.95
20:49:00	320	06:39:53	23,993	3.84
20:59:30	290	06:50:23	24,623	3.75
21:08:30	276	06:59:23	25,163	3.67
21:15:30	264	07:06:23	25,583	3.61
21:21:10	244	07:12:03	25,923	3.56
21:25:20	228	07:16:13	26,173	3.52
21:25:20	220	07:16:13	26,173	3.52
21:20:50	216	07:11:43	25,903	3.56
21:17:00	192	07:07:53	25,673	3.59
21:14:30	168	07:05:23	25,523	3.61
21:12:00	158	07:02:53	25,373	3.64
21:10:05	148	07:00:58	25,258	3.65
21:08:40	131	06:59:33	25,173	3.66
21:07:40	108	06:58:33	25,113	3.67
		R_7—Δ = 132,270 km.		
24:28:40	223	10:19:33	37,173	3.55

[a] Clock correction, + 23 sec.

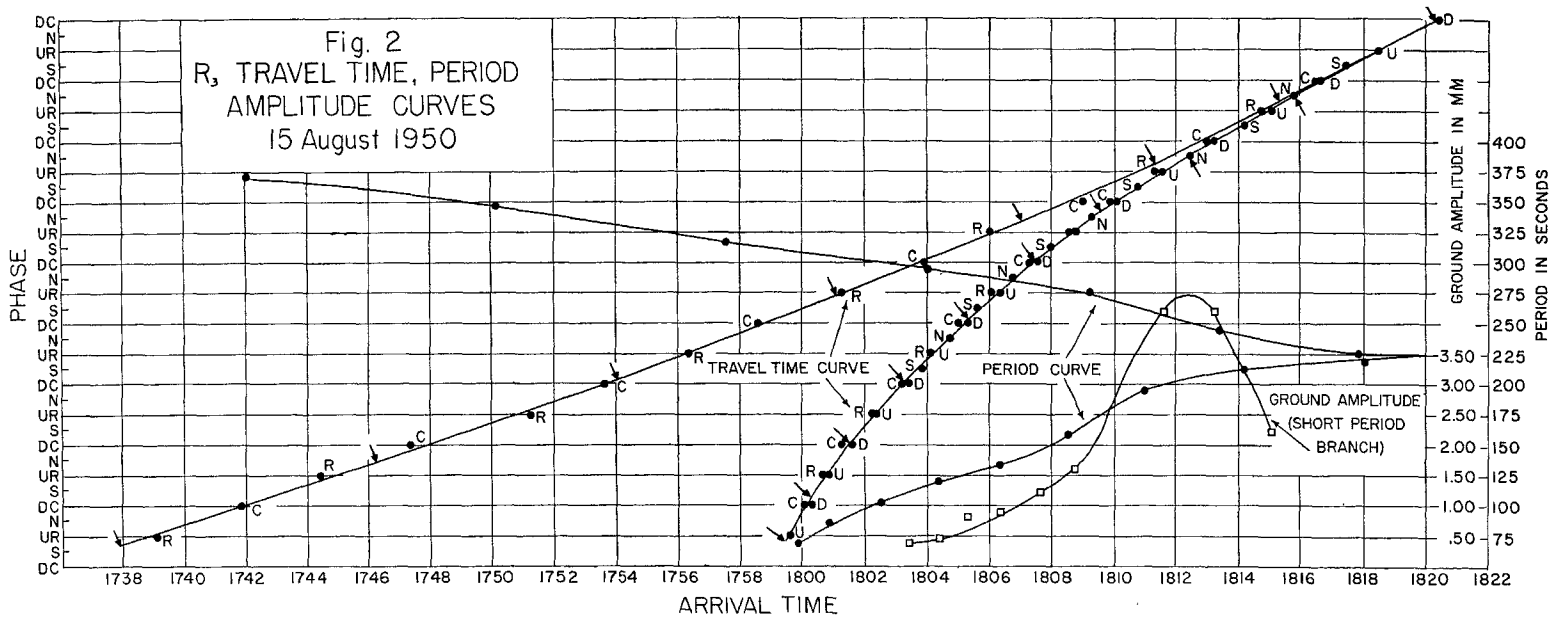

Fig 2. Arrival-time, period, and amplitude curves for R_3 waves from the earthquake of 15 August 1950.

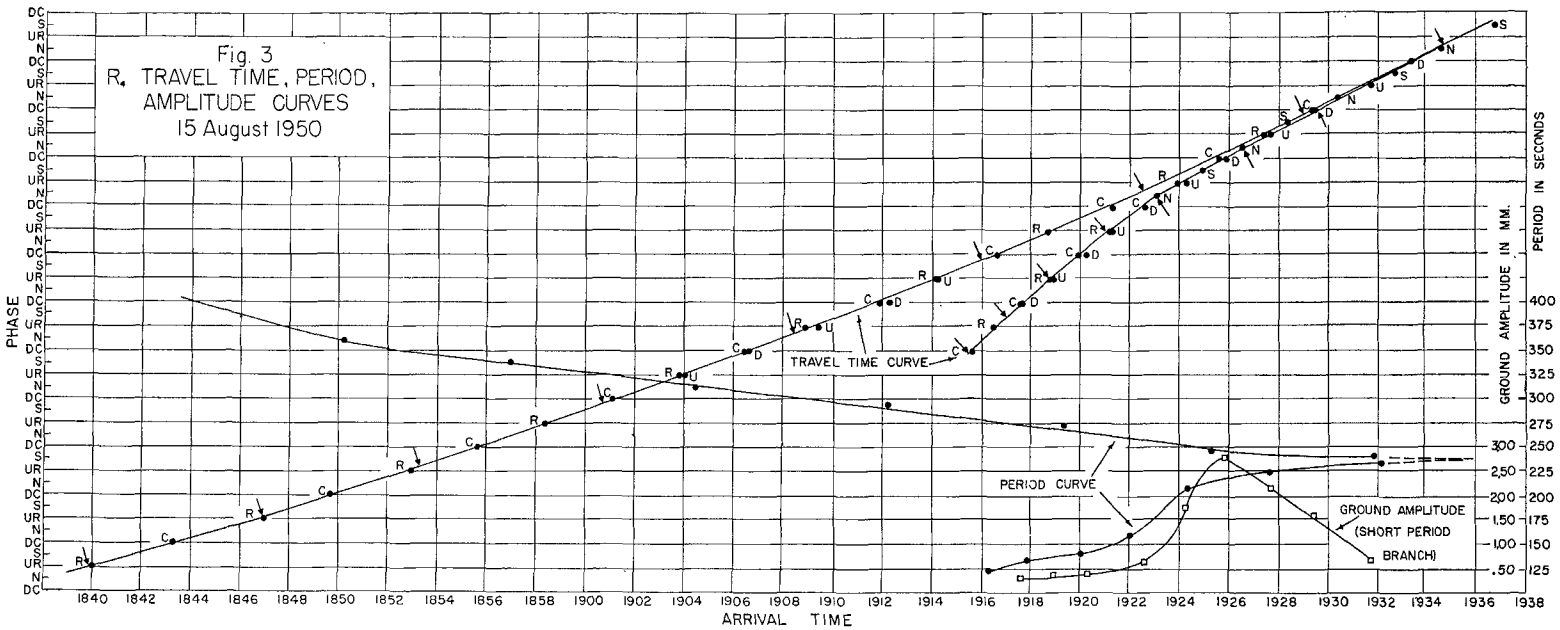

Fig. 3. Arrival-time, period, and amplitude curves for R_4 waves from the earthquake of 15 August 1950.

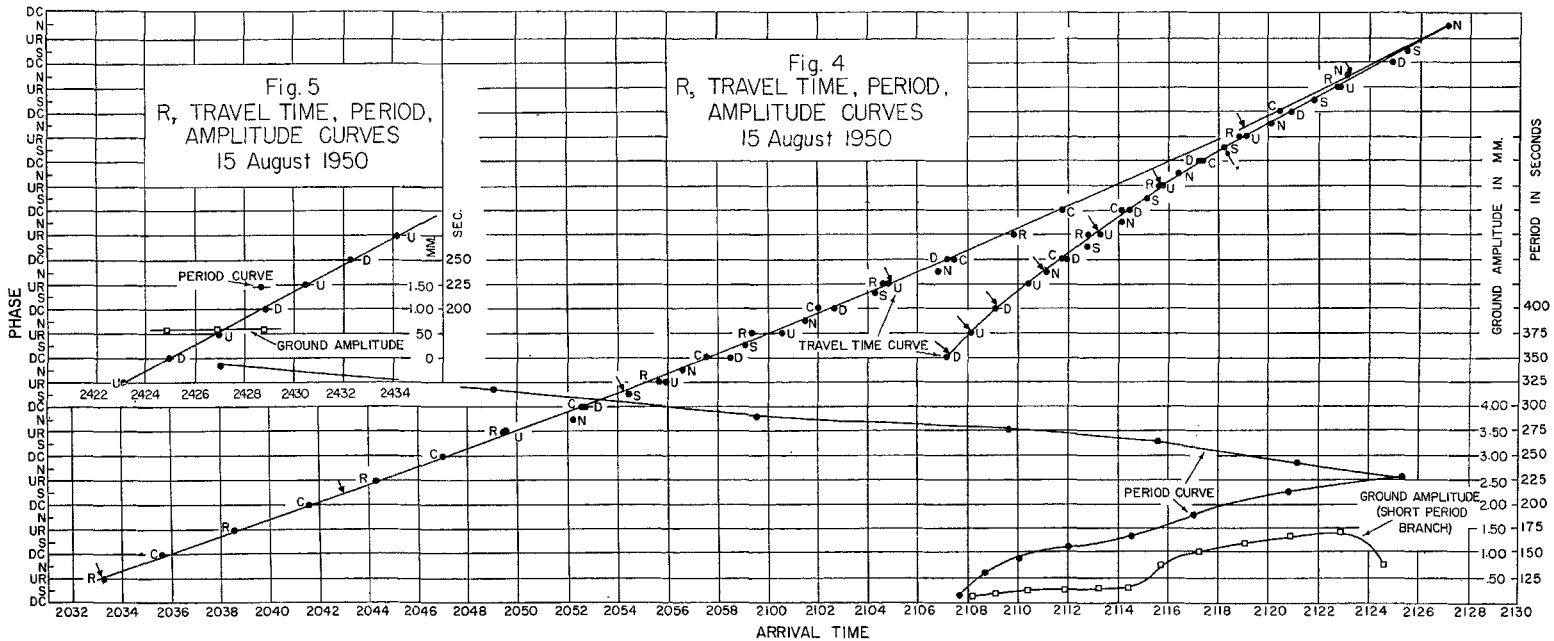

Fig. 4. Arrival-time, period, and amplitude curves for R_6 waves from the earthquake of 15 August 1950.
Fig. 5. Arrival-time, period, and amplitude curves for R_7 waves from the earthquake of 15 August 1950.

figures 2–5. The abscissas are arrival times, and the ordinates to the left represent the phase of the oscillations, one space representing one-half cycle. The small arrows represent the limits of the straight-line segments with which each curve was approximated. The slope and midpoint of each straight-line segment were read from these graphs, and from them the arrival times for waves of each period were computed. These results are plotted on the same graphs as period curves. Travel time and group velocity were then computed for each period. The resulting dispersion data for each order of Rayleigh waves appear in table 5.

TABLE 6

ARRIVAL TIMES FOR MAXIMUM AND MINIMUM TRACE DEFLECTIONS, 2 MARCH 1933

Short-period branch		Short-period branch		Short-period branch	
R_2 phase	Uncorrected arrival time (P.S.T.)	Uncorrected R_3 phase	Uncorrected arrival time (P.S.T.)	Uncorrected R_4 phase	Uncorrected arrival time (P.S.T.)
C	11:48:10	C	13:05:33	R	15:01:53
R	48:48	R	13:06:34	C	15:03:22
C	49:43	C	07:35	R	15:05:10
R	50:33	R	08:40	R	15:05:10
C	51:12	C	09:45	C	15:06:52
R	51:46	R	11:06	R	15:09:11
C	52:32	C	12:21		
R	53:26	R	13:28		
C	54:19	C	15:00		
R	55:23	R	16:40		
C	56:29	C	19:06		
R	57:45				
C	59:06				
R	12:00:54				
C	12:02:25				
R	12:04:43				

It will be noted that each of these arrival-time and period curves (except R_7) has first a long-period branch, representing a train of waves whose period decreases with time. The long-period branch is interrupted abruptly by a train of much shorter waves in which the period increases with time. In many cases it is possible to read the long-period waves for several cycles following the onset of the short-period waves; but, as is usual when working near a minimum value of group velocity, one cannot read both branches to the point where the periods are equal. This gap in readings might suggest that there is arbitrary choice in fitting the ordinates of each short-period branch of the arrival-time curves to the long-period branches, but the gap is too short to permit uncertainty.

Arrival times for maximum and minimum trace deflections of R_2, R_3, and R_4 waves are plotted in table 6 for the earthquake of 2 March 1933. Dispersion data are given in table 7. Table 8 gives the corresponding data for R_2 waves from the earthquake of 8 September 1948. These data are depicted in graphical form in figures 6 and 7. Group velocity as a function of period for all observed orders of Rayleigh waves is presented in figure 8. The dotted part of the curve represents the

portion which is unobservable owing to the overlapping of the two branches. It is easily seen in figures 2–4 that the choice of ordinates which was made produces a reasonable shape for the dotted part of the dispersion curve, which is demanded by the character of R_7.

It can be seen that a single dispersion curve represents all the orders and that there

TABLE 7
DISPERSION DATA, 2 MARCH 1933

Uncorrected arrival time[a] (P.S.T.)	Period (sec.)	Travel time (sec.)	Velocity (km/sec.)
	R_2		
11:52:10	96.5	8457	3.76
53:08	106	8515	3.73
54:00	112	8567	3.71
55:00	124	8627	3.69
56:10	133	8697	3.66
57:20	154.5	8767	3.63
59:10	189	8877	3.58
12:01:35	225	9022	3.52
	R_3		
13:06:00	120	12887	3.75
13:07:30	126	12977	3.72
13:08:55	138	13062	3.70
13:10:25	144	13212	3.65
13:12:10	158	13257	3.64
13:13:55	176	13362	3.61
13:15:40	206	13467	3.58
13:17:30	232	13577	3.55
	R_4		
15:02:50	192	19897	3.61
15:05:10	220	20037	3.58
15:07:55	252	20202	3.56

[a] Clock correction, −12 sec.

is no indication whatever of a systematic shift of this curve with increasing length of path. It is also evident that the spectra of the various Rayleigh-wave trains are determined primarily by dispersion since R_3, R_5, and R_7 cover progressively narrower period ranges centering about 225 sec., the period for minimum group velocity. This agrees with the well-known relation between amplitude and the slope of the group velocity curve. Analagous results have been obtained in propagation of explosion sounds in shallow water.[3]

[3] M. Ewing, J. L. Worzel, and C. L. Pekeris, "Propagation of Sound in the Ocean," *Mem. Geol. Soc. Am.*, Vol. 27 (1948).

For the earthquake of 15 August 1950, R_4 was observable for a period range almost as long as that for R_3. This probably results from the fact that the seismogram in the neighborhood of R_3 is still considerably disturbed by short-period surface waves, but the possibility of an azimuthal dependence cannot be entirely ruled out. Observations of R_6 would have settled this point, but unfortunately the seismograms are unreadable during the interval 22:09 to 22:50, owing to artificial disturbance.

The remarkable agreement of the dispersion for the various orders of Rayleigh waves suggests that scattering effects are negligible in the propagation of mantle

TABLE 8

R_2 ARRIVAL TIMES AND DISPERSION DATA, 8 SEPTEMBER 1948

(Δ = 31,470 km.)

Phase	Uncorrected time[a] (G.C.T.)	Uncorrected arrival time[a] (G.C.T.)	Period (sec.)	Travel time (sec.)	Velocity (km/sec.)
U		17:25:25	59	8178	3.85
D	17:25:05	17:26:50	90	8263	3.81
U	25:35	17:29:20	113	8413	3.74
D	26:10	17:32:05	136	8578	3.67
U	26:55	17:34:35	198	8728	3.61
D	27:40				
U	28:35				
D	29:35				
U	30:25				
D	31:30				
U	32:40				
D	34:05				
U	35:40				

[a] Clock correction, +7 sec.

Rayleigh waves. Absorption studies on these waves should yield data on elastic imperfection in the mantle with a higher degree of precision than was available in earlier investigations of shorter-period waves where scattering could not be estimated. Earlier investigations suffer from the added difficulty that waves of a given period could not be followed over the wide range of distances available in this study.

AMPLITUDES

In tables 1–4, peak-to-peak ground amplitudes are listed as a function of arrival time for the short-period branches of R_3, R_4, R_5, and R_7 waves from the earthquake of 15 August 1950. These data, together with periods, are plotted as a function of arrival time in figures 2–5. From these graphs ground amplitudes were obtained as a function of period; the data appear in table 9, and the amplitudes are plotted in figure 9. It is seen that the maximum amplitudes fall between 205 and 225 seconds, reasonably close to the period of minimum group velocity. Amplitudes could be read with precision only for these waves, the relatively high background preventing similar treatment for the long-period branch and for the waves from the other shocks.

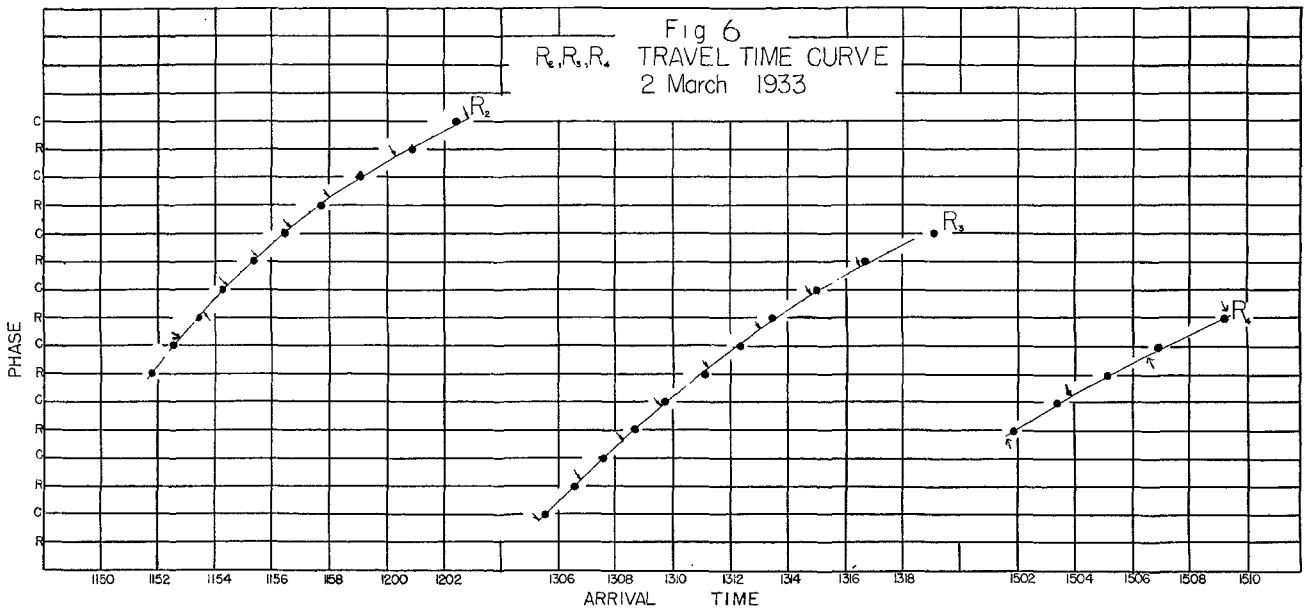

Fig. 6. Arrival-time curves for R_2, R_3, R_4 waves from the earthquake of 2 March 1933.

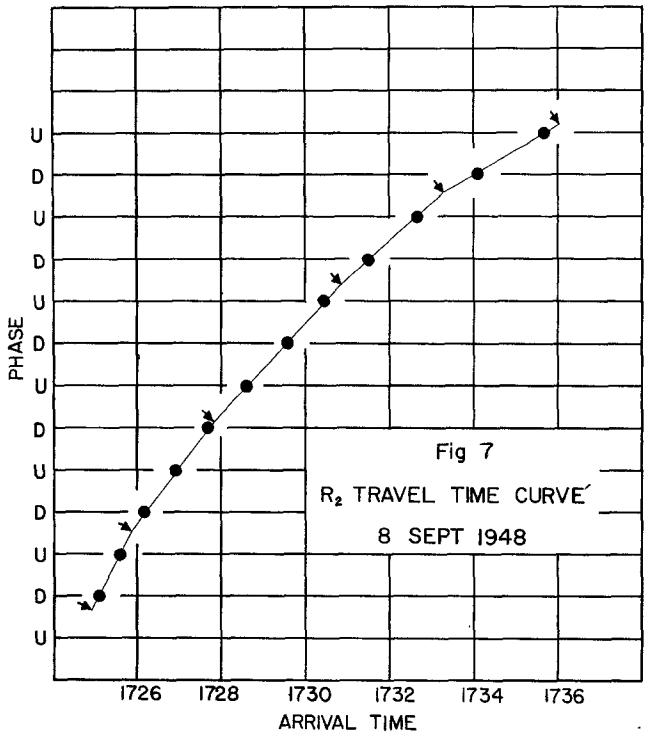

Fig. 7. Arrival-time curve for R_2 waves from the earthquake of 8 September 1948.

TABLE 9

GROUND AMPLITUDES FOR VARIOUS PERIODS, 15 AUGUST 1950

R_3 short-period branch		R_4 short-period branch		R_5 short-period branch		R_7	
T	Ground ampl. (mm.)	T	Ground ampl. (mm.)	T	Ground ampl. (mm.)	T	Ground ampl. (mm.)
110	0.40	138	0.40	122	0.16	223	0.60
131	0.74	145	0.48	150	0.28		
150	1.3	160	0.60	160	0.32		
180	2.6	175	0.76	167	0.36		
192	3.5	202	1.4	178	0.76		
205	4.5	217	2.8	200	1.1		
209	4.1	225	2.1	210	1.2		
212	3.2	230	1.3	221	1.4		
215	2.2	233	0.80	227	0.74		

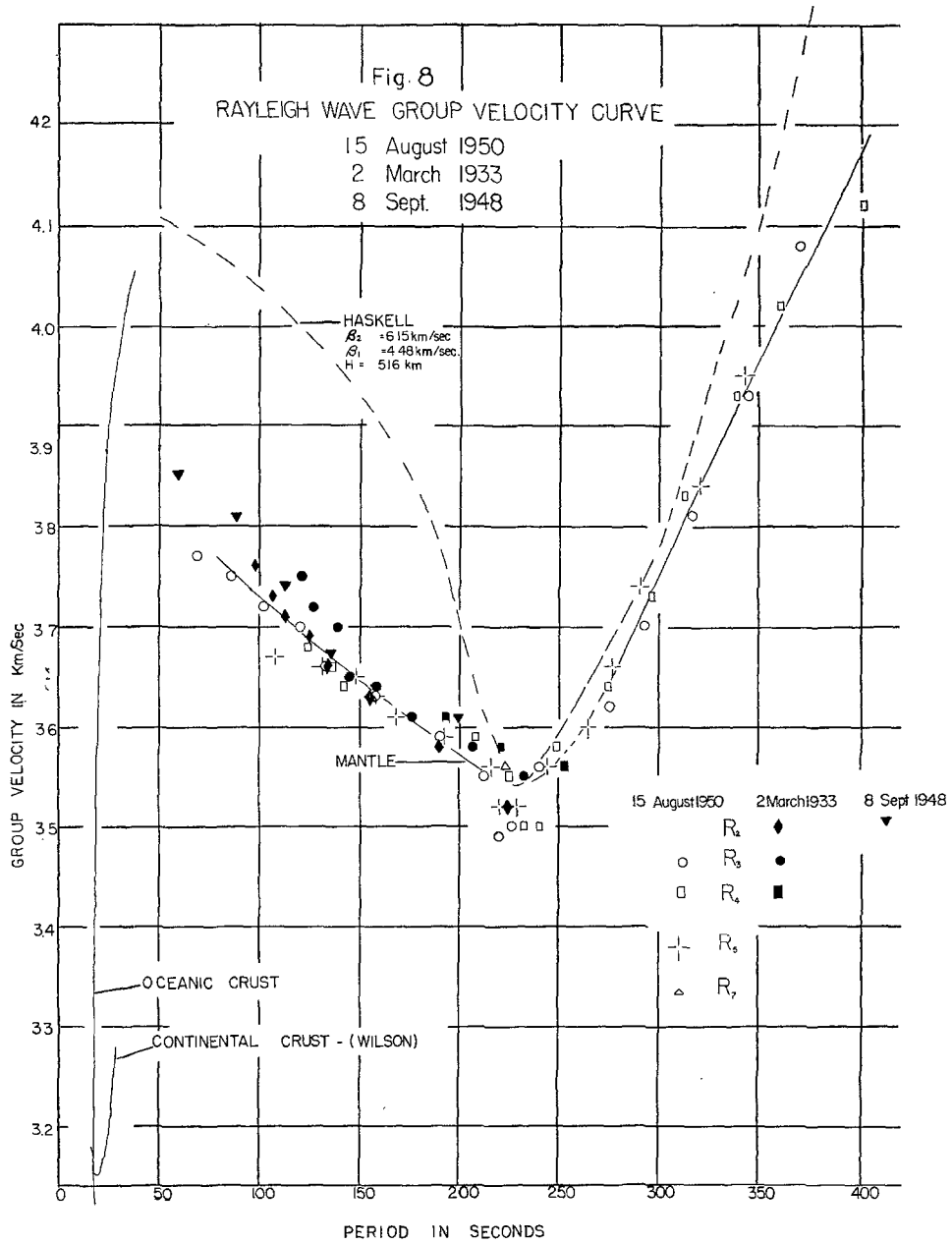

Fig. 8. Observed group velocity curve for mantle Rayleigh waves compared to theoretical curve based on single-layer approximation.

Since the effect of geometrical spreading is a constant for the various orders of Rayleigh waves, at a given station the amplitude for the Airy phase will vary approximately as $e^{-\gamma\Delta}/\Delta^{1/3}$. In a similar manner the amplitude for any other period in the wave train will vary as $e^{-\gamma\Delta}/\Delta^{1/2}$. Here γ represents the loss due to dissipation effects, and the factors $\Delta^{1/3}$ and $\Delta^{1/2}$ represent the effect of dispersion or "stretch-

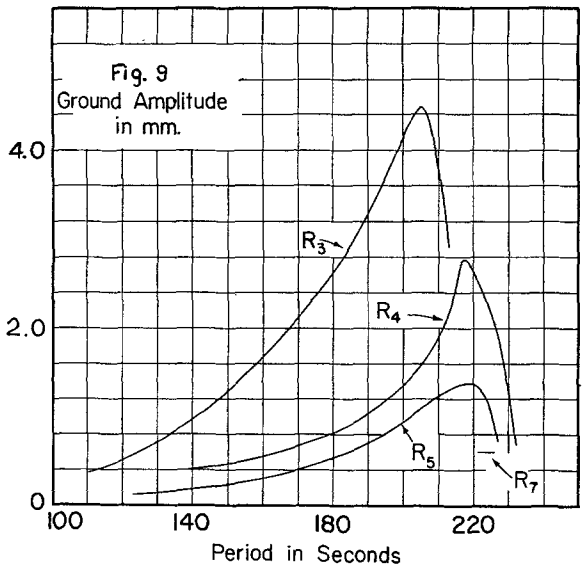

Fig. 9. Vertical ground amplitudes (peak to peak) for short-period branch of R_3, R_4, R_5, R_7 waves as a function of period for the earthquake of 15 August 1950.

ing" of the wave train. The exponents of Δ given above ignore an effect of sphericity but are considered satisfactory for an approximate calculation. Although not needed for study of a single station, approximate allowance for the effect of geometrical spreading is made by the factor $(\Gamma_0 \sin \Delta)^{-1/2}$, where Γ_0 is the earth's radius, except for Δ near to 0, π, 2π etc. Thus we will use the relations

$$A = \frac{\bar{A}_0 e^{-\gamma\Delta}}{|\Gamma_0 \sin \Delta|^{1/2} \Delta^{1/3}} \tag{1}$$

for the Airy phase and

$$A = \frac{A_0 e^{-\gamma\Delta}}{|\Gamma_0 \sin \Delta|^{1/2} \Delta^{1/2}} \tag{2}$$

for other periods in the wave train.

From the amplitude vs. period curves of figure 9 the constants A_0 and γ are readily determined for a given period by making a plot of $ln(A \cdot \Delta^{1/3})$ against Δ for the Airy phase or $ln(A \cdot \Delta^{1/2})$ for the other waves. Such a graph is presented in figure 10. It is seen that the data for $T = 140$ sec., 180 sec., and 215 sec. (Airy phase) can be represented by the two straight lines indicated. These lines give the relations

$$A_z = \frac{104}{\Delta^{1/3}} e^{-.0024\Delta} \qquad \text{for } T = 215 \text{ sec.} \tag{3}$$

and

$$A_z = \frac{144}{\Delta^{1/2}} e^{-.0040\Delta} \qquad \text{for } T = 140 \text{ sec.} \tag{4}$$

The absorption coefficients .0024 deg.$^{-1}$ (.0000216 km.$^{-1}$) and .0040 deg.$^{-1}$ (.0000360 km.$^{-1}$) thus determined show that the amplitudes of mantle Rayleigh waves decrease by two-fifths for $T = 215$ sec. and by one-fourth for $T = 140$ sec. owing to absorption alone for each circuit of the earth.

A simple computation indicates that if viscosity is to account for the absorption, a value of the order of 10^{15}–10^{16} poises is needed in the upper mantle. Since this is many orders of magnitude less than the values 10^{20}–10^{22} poises given by the occur-

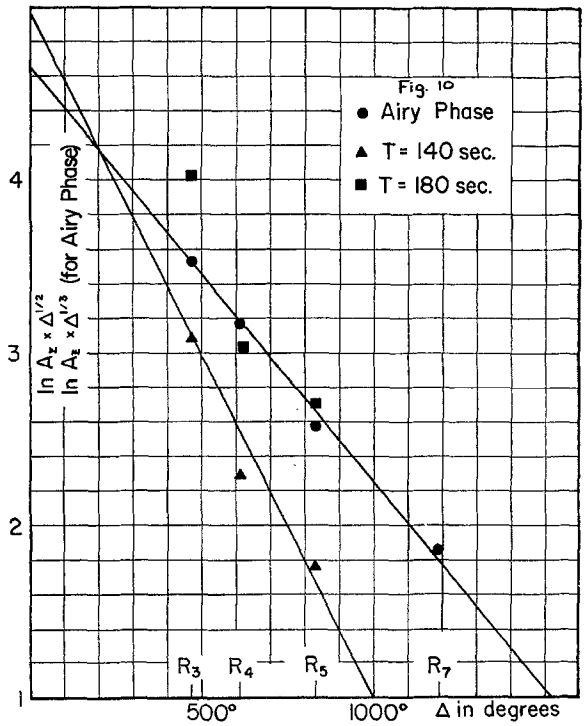

Fig. 10. Graph of logarithm of product of ground amplitude and dispersion factor to obtain constants A_0, $\overline{A}_0$, and γ.

rence of deep-focus earthquakes and the recoil of the earth after the disappearance of the Pleistocene ice in Fennoscandia,[4] the absorption can be ascribed to the effect of internal friction.

The internal friction may be specified by a dimensionless parameter Q[5] related to the absorption coefficient γ by the equation

$$\gamma = \pi/QcT \tag{5}$$

where c is phase velocity and T is period.

In general Q is a function of vibration amplitude, period, temperature, mechanical and thermal treatment, and chemical impurity, among other factors. For

[4] *Internal Constitution of the Earth* (2d ed.; New York, Dover Publications, 1951), chap. xv.
[5] See, for example, Birch, *Handbook of Physical Constants*, Geol. Soc. Am. *Spec. Paper 36* (1942).

a given material, however, in a given physical state, Q may be taken approximately as independent of the period. In porous media such as rocks, the dissipation is decreased by compression, resulting in an increase of Q with pressure.

From the values given above and from equation 5 we find

$$1/Q = 665 \times 10^{-5} \quad \text{for} \quad T = 215 \text{ sec.}, c = 4.5 \text{ km/sec.}$$
$$1/Q = 673 \times 10^{-5} \quad \text{for} \quad T = 140 \text{ sec.}, c = 4.2 \text{ km/sec.}$$

These may be compared to the values[6] $1{,}000 \times 10^{-5}$ and 80×10^{-5} for Quincy granite at a pressure of 1 atmosphere and 4,000 atmospheres respectively, obtained from laboratory studies of the logarithmic decrement of free vibrations at audio frequencies. The corresponding values for Vinal Haven diabase are 170×10^{-5} at 1 atmosphere and 280×10^{-5} at 4,000 atmospheres. It is surprising that the values of internal friction determined in this way for the upper mantle are of the same order of magnitude as that found in the laboratory vibration measurements on crystalline rocks at audio frequencies.

Since depth of effective penetration of mantle Rayleigh waves increases with period, study of the variation of mantle structure with depth is feasible by this technique. Improved instrumentation will be required to extend the period range. Use of mantle Love waves (G waves) for which the penetration dependence on period varies differently may aid in the difficult probelm of evaluating effects on Q of pressure and temperature of mantle rocks, as well as wave periods.

Discussion

Near the left side of figure 8 are shown in full lines the dispersion curves for oceanic paths as given by Ewing and Press[7] and for continental paths as given by Wilson and Baykal.[8] These are theoretical curves which are well supported by observation. The oceanic curve is calculated for an ocean layer 5.57 km. thick over an extended solid substratum with shear velocity $\beta_2 = 4.56$ km/sec. and density $\rho_2 = 3.0$ gm/cm^3. The continental curve is calculated for a layer 37 km. thick with $\beta_1 = 3.7$ km/sec. overlying an extended substratum with $\beta_2 = 4.45$ km/sec. and $\rho_2/\rho_1 = 57/50$. The theoretical extensions of the continental and oceanic dispersion curves to periods longer than those for which observations have been available approach the value $.92\beta_2$. These theoretical extensions assume that the substratum extends to infinite depth without change of properties. Under these conditions the asymptotic value of group velocity for long waves is about 4.2 km/sec. The asymptotic value is approached for shorter periods by the oceanic curve than by the continental curve, the controlling layer being much thinner for the former case. But for periods greater than about 60 sec. the two curves are approximately the same.

The marked deviation from these extended theoretical curves shown by the observations reported here of group velocity for longer periods is simply due to the fact that the long waves are reaching to depths where a change in the properties of the substratum is encountered. It will be shown by an approximate calculation that the necessary change in properties is consistent with the known properties of the mantle,

[6] See *ibid.*
[7] See note 2 above.
[8] See note 1 above.

and the long-period Rayleigh waves will be referred to as mantle Rayleigh waves to distinguish them from the shorter-period crustal Rayleigh waves.

The period range between 40 sec. and 70 sec. is lacking in observations and corresponds to the transition from crustal to mantle propagation. The 70-sec. curves which mark the short-wave limit for mantle propagation are considered to be the shortest waves which are free from strong scattering and refraction at the major crustal discontinuities between oceans and continents, and hence the absence of shorter periods from the higher order paths is expectable.

The absence of longer periods from R_1 and R_2 is a less definite matter. It is related to masking by the crustal Rayleigh waves to which the instruments are more sensitive and to the distance required for adequate spreading of the wave train.

Two-layer approximation.—The calculations for a theoretical Rayleigh-wave dispersion curve for periods up to 7 minutes for the known velocity and density distribution in the crust and mantle down to 1,500 kilometers are prohibitive if present methods are used, the principal complication arising from the gradual increase of velocity with depth. The inverse problem of calculating the velocity-depth relation from the dispersion observations is even more difficult. As a first approximation a greatly simplified structure which is suggested by a calculation of Pekeris[9] will be assumed.

Pekeris chose two liquid layers with thicknesses h_1 and h_2 over an extended liquid substratum and obtained the appropriate dispersion curve. He made two auxiliary calculations: (*a*) a single-layer case in which h_2 is infinite, (*b*) a single-layer case in which h_1 is absent, and found that if the large ratio $h_2/h_1 = 10$ is taken, the three-layer problem may be adequately represented by these separate single-layer problems, greatly simplifying the calculations.

This suggests that crustal and mantle Rayleigh-wave observations may likewise be represented by two separate single layer problems, as follows:

1) The continental or oceanic crust will be represented by a single homogeneous layer underlain by a homogeneous mantle of infinite extent, being the same in all respects as the previous solutions for crustal Rayleigh waves as shown at the left side of figure 8. A still better approximation would make use of the recent treatment by Newlands[10] of Rayleigh waves in a two-layer heterogeneous medium with different values of the elastic parameters in order to secure a better fit with observed dispersion than she was able to do.

2) The mantle, in which it is known from body-wave studies that the velocity increases gradually with depth, is approximated as a single-layer problem with the constants $\beta_2 = 6.15$ km/sec., $\alpha_2 = 10.93$ km/sec., $\beta_1 = 4.48$ km/sec., $\alpha_1 = 8.11$ km/sec., $\rho_2/\rho_1 = 1.11$, $H = 516$ km. The dispersion curve for this layering may be obtained from the computations by Haskell[11] for Rayleigh-wave propagation in multilayered media. The value of β_1 was taken to be close to that derived for the substratum in the studies of crustal Rayleigh waves. H was selected to make the period of the point of minimum group velocity coincide with the observed Airy phase (225 sec. and 3.54 km/sec.). The calculated dispersion curve is shown in

[9] See note 3 above.

[10] Margery Newlands, "Rayleigh Waves in a Two-layer Heterogeneous Medium," *Mon. Not. Roy. Astron. Soc., Geophys. Suppl.*, 6: 109–128 (1950).

[11] Norman Haskell, "The Dispersion of Surface Waves on Multilayered Media," *Bull. Seism. Soc. Am.*, 43: 17–34 (1953).

figure 8. The curve is not a good fit, but it shows that the general trend of the observed curve can be explained as a minimum of group velocity caused by increase of shear-wave velocity with depth in the mantle. It is considered probable that a better fit could be obtained if calculations were available for a structure resembling the actual mantle more closely. Again the results of Newlands could be used to compute better approximations.

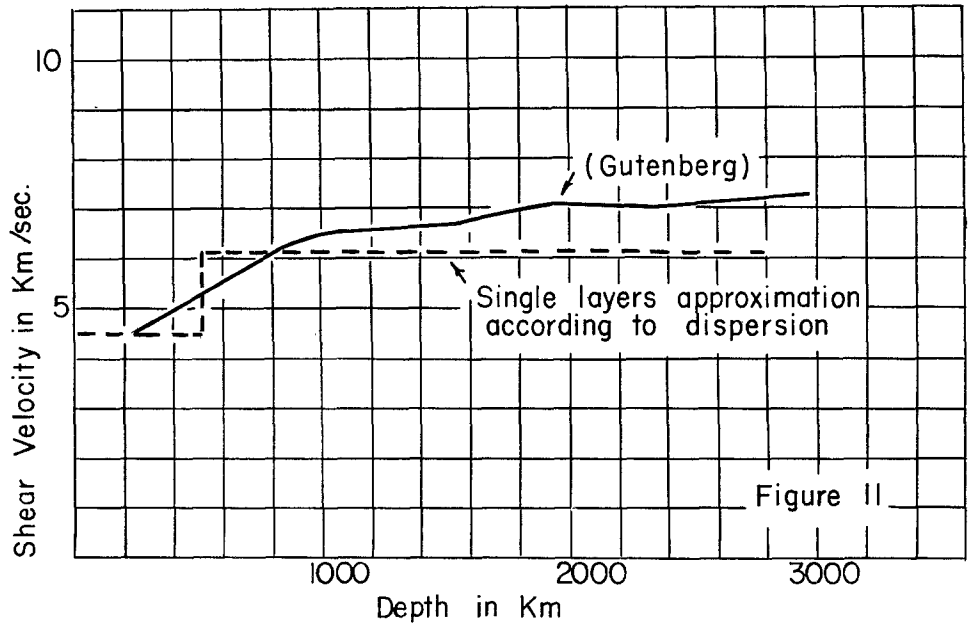

Fig. 11. Comparison of shear-wave variation with depth according to Gutenberg, and single-layer approximation deduced from mantle Rayleigh-wave dispersion.

Referring to figure 11, where the velocity-depth curve of Gutenberg is shown, it is seen that the velocity-depth relation deduced from the highly simplified one-layer dispersion calculation is in reasonably good agreement.

Conclusions

An investigation of mantle Rayleigh waves from three earthquakes has resulted in a group velocity curve with data from R_2, R_3, R_4, R_5, and R_7 waves showing surprisingly little scatter. The group velocity curve has a definite minimum value at a period of 225 sec. and velocity of 3.54 km/sec. It is suggested that the known variation of shear-wave velocity with depth in the mantle can account for the observed dispersion. The small scatter in velocity for the large range of distances and the different paths indicates that the scattering and refraction effects at continental margins and differences between oceanic and continental crustal structure have no influence on the propagation of these waves. For this reason the value of $1/Q = 670 \times 10^{-5}$ deduced for the internal friction in the upper mantle for waves of periods 140–225 sec. is believed to be a fairly accurate determination.

Lamont Geological Observatory
(Columbia University)
Contribution No. 107